Food Research International 99 (2017) 730–738

Contents lists available at ScienceDirect

Food Research International

journal homepage: www.elsevier.com/locate/foodres

Comparative analysis of *C*-glycosidic flavonoids from *Prosopis* spp. and *Ceratonia siliqua* seed germ flour

Gianluca Picariello[a,*], Leonardo Sciammaro[b], Francesco Siano[a], Maria Grazia Volpe[a], Maria Cecilia Puppo[b,*], Gianfranco Mamone[a]

[a] Istituto di Scienze dell'Alimentazione, Consiglio Nazionale delle Ricerche (CNR), Via Roma 64, I-83100 Avellino, Italy
[b] Centro de Investigación y Desarrollo en Criotecnología de Alimentos (CIDCA – UNLP – CONICET), Calle 47 y 116, 1900 La Plata, Argentina

ARTICLE INFO

Keywords:
Prosopis spp.
C. siliqua
Seed germ
Apigenin *C*-glycosides
High resolution MS/MS
α-glucosidase inhibitors

ABSTRACT

Seed germ of South American algarrobo (*Prosopis* species) and European carob (*Ceratonia siliqua*) contains nutritionally interesting proteins, lipids and phenolics. Using reversed phase-HPLC-diode array detector and nanoflow-HPLC coupled to tandem mass spectrometry (MS/MS), we comparatively characterized and semi-quantified flavonoids from germ of three Argentinean algarrobo (*Prosopis alba*, *Prosopis nigra* and *Prosopis ruscifolia*) and one European carob species. The patterns of glycosylated flavonoids were very similar each other, confirming the taxonomic parentage of the species and supporting their functional similarity on a molecular basis, in view of the use of seed germ flour (SGF) for food applications. The predominant phenolic compounds were apigenin 6,8-*C*-di-glycoside isomers, namely isoschaftoside and schaftoside, accounting for 3.22–5.18 and 0.41–0.72 mg/g SGF, respectively. *C. siliqua* germ contained relatively high amounts of further glycosilated derivatives of (iso)schaftoside, which occurred at a lower abundance in *Prosopis*. Apigenin 6,8-*C*-di-glycosides have been described as potent α-glucosidase inhibitors, suggesting that food preparations obtained with *Prosopis* spp. and *C. siliqua* SGF might contribute to modulate the digestion of carbohydrates in humans.
Chemical compounds: Isoschaftoside (PubChem CID: 13644661); Schaftoside (PubChem CID: 442658); Vicenin-2 (PubChem CID: 442664); Isovitexin (PubChem CID: 162350).

1. Introduction

Prosopis spp. is a genus of *Fabaceae* (*Leguminosae*) comprising around 45 species distributed in the subtropical or tropical regions of America, Africa and Asia. Argentina ranks first for the biodiversity of *Prosopis* spp., accounting for nearly 27 catalogued biotypes (Burkart, 1976). *Prosopis* genus comprise xerophyte trees or shrubs, enduring high temperatures, drought, alkalinity and salinity, besides exhibiting high capability of nitrogen fixation (Villagra et al., 2004). Among the varieties used for human consumption, *P. alba* and *P. nigra* are commonly known as algarrobo, whereas *P. ruscifolia*, a colonizer shrubby tree is referred as vinal (Freyre et al., 2003). All these species grow in dry areas of the Argentinean North-West known as Argentine Espinal (Cabrera, 1976).

The algarrobo (or vinal) pods and derived products are associated by native communities of the Northern Argentina to their own identity and peculiarity. Aborigine people have traditionally used algarrobo trees, especially *P. chilensis* and *P. flexuosa,* as a source of wood for construction or for burning. The edible pods of *P. alba* and *P. nigra* have been largely used for food and feed purposes (Choge et al., 2007; Sciammaro, Ribotta, & Puppo, 2016). *Prosopis* spp. pods are consumed as fruits or are ingredients of different traditional products like “añapa” (sweet non-fermented, nonalcoholic beverage) or “aloja” (sweet fermented-alcoholic beverage). Pods can be roasted, grinded and incorporated to milk as well. Native people are used to save algarrobo pods in “trojas” (saddlebag or slammer) or covert them into different products, such as flour, “patay” (pressed cake), “arrope” (syrup) and “bolonchao” (Sciammaro, Ferrero, & Puppo, 2016).

Ceratonia siliqua L. (carob) is a typical Mediterranean tree also belonging to the *Fabaceae* family, sharing morphological and compositional similarity with *Prosopis* spp. plants. Carob has been cultivated for centuries especially in Spain, Italy, Portugal and Morocco because of its edible fruits (Ayaz et al., 2009). The non-fleshy and bean-like carob pods are utilized in many Arabian countries for popular beverages and confectionery (Yousif & Alghzawi, 2000). In Sicily, the carob pod meal has been used in the past for human nutrition and to prepare

* Corresponding authors.
E-mail addresses: picariello@isa.cnr.it (G. Picariello), sciammaro@gmail.com (L. Sciammaro), francesco.siano@isa.cnr.it (F. Siano), mgvolpe@isa.cnr.it (M.G. Volpe), mcpuppo@quimica.unlp.edu.ar (M.C. Puppo), mamone@isa.cnr.it (G. Mamone).

http://dx.doi.org/10.1016/j.foodres.2017.06.058
Received 21 April 2017; Received in revised form 23 June 2017; Accepted 25 June 2017
Available online 27 June 2017

homemade cakes, although often restricted to periods of food shortage. Because of the relatively high content of sugar, mainly sucrose, flours of roasted pods from both algarrobo and carob constitute natural sweeteners, commonly employed as cacao and coffee surrogates, which do not contain excitant substances such as caffeine and theobromine (Bengoechea et al., 2008). The excellent flavoring properties in terms of both taste and aroma render flours adequate ingredients for pastries, muffins and biscuits (Bigne, Puppo, & Ferrero, 2016; Salinas, Carbas, Brites, & Puppo, 2015). Carob and algarrobo flours have been proposed and are increasingly used as a suitable ingredient to produce gluten-free baked products.

In the traditional uses of carob, seeds are generally discarded. Nowadays, carob seeds are utilized in food industry to obtain locust bean gum (LBG), which is a galactomannan used as a natural additive (E 410) with excellent texturing and thickening properties (Avallone, Plessi, Baraldi, & Monzani, 1997; Srivastava & Kapoor, 2005). *Prosopis* seeds are not generally processed to obtain gum, although composition of the seed endosperm is similar to that of *C. siliqua* (Bush, Kolender, Santagapita, & Bluera, 2015; Saunders & Becker, 1989).

Germ is the by-product remaining after removal of the seed cuticle and the inner gum layer. Seeds account for 10–15% in weight of the algarrobo and carob pods, germ representing nearly half of the seed weight (Sciammaro, Ferrero, & Puppo, 2016). Based on preliminary investigations, germ contains several functionally and nutritionally interesting components, including proteins, lipids and phenolics (Custódio et al., 2011; Sciammaro, Ferrero, & Puppo, 2016; Sciammaro, Ribotta, & Puppo, 2016). By virtue of exclusive nutrient composition and nutritional properties, seed germ flour (SGF) from both *C. siliqua* and *Prosopis* samples has potential to be used as an ingredient for special food formulations (Bengoechea et al., 2008; Dakia, Wathelet, & Paquot, 2007; Sciammaro, Ribotta, & Puppo, 2016). The preparation of gluten-free baked products using flour obtained from seeds (germ and endosperm) of vinal is particularly interesting, as it contains > 50% (*w*/w) of galactomannans, which improve the rheological properties of the gluten-free dough (Bernardi, Sánchez, Freyre, & Osella, 2010; Bush et al., 2015).

However, the composition of SGF still awaits to be characterized at a molecular level. Germ is light-yellow colored, with honey or golden shades, suggesting the presence of pigments. Unlike the phenolic constituents of pods from both carob (for a list of relevant studies see Karim & Azlam, 2012) and algarrobo (Pérez et al., 2014), which have been characterized for their potential bioactive properties, to the best of our knowledge very limited information is available about the polyphenol constituents of germ. In a very recent paper, apigenin *C*-glycosides have been described as the main polyphenols of *P. alba* cotyledons (Cattaneo et al., 2016), in agreement with those characterized many years ago in the cotyledon of *C. siliqua* (Batista & Gomez, 1993 and references therein).

In this work, we comparatively analyzed the polyphenol extracts from SGF of *P. alba*, *P. nigra*, *P. ruscifolia* and *C. siliqua*, using reversed phase-high performance liquid chromatography (RP-HPLC) with diode array detection (DAD) and nanoflow-HPLC coupled to positive and negative ion mode high resolution electrospray ionization (ESI) tandem mass spectrometry (MS/MS). Major components were semi-quantified by RP-HPLC. The detailed knowledge of SGF phytochemical composition will contribute to define their potential use for functional foods and nutraceutical preparations.

2. Materials and methods

Standard apigenin, trifluoroacetic acid (TFA), formic acid, HPLC-MS grade water, methanol and acetonitrile were from Sigma-Aldrich (St. Louis, MI, USA).

2.1. Seed germ samples

Prosopis alba, *nigra* and *ruscifolia* pods were collected in Santiago del Estero (Argentina) between 2010 and 2014. Seeds were hulled from pods and were soaked in boiling water, left to cool at room temperature and then rested in water overnight at 4 °C to enable the separation of the different seed compartments. After hydration, epicarp, endosperm and germ from *Prosopis* spp. seeds were manually separated as previously detailed (Sciammaro, Ferrero, & Puppo, 2016). Germ was obtained free from other compartments, after careful removal of the LBG envelope. Isolated germ specimens were freeze-dried, ground into a fine flour (SGF) and stored at − 20 °C. Carob protein isolate obtained from *Ceratonia siliqua* seed germ was supplied by a Spanish company of plant proteins (PEVESA Biotech, Spain). The protein content of the isolate was 89.9 wt% (d.b.) and moisture was 10.8%, according to the label.

2.2. Polyphenol extraction

SGF samples (100 mg) were sequentially extracted with 1 mL methanol, 1 mL 80% aqueous methanol (v/v) and 1 mL 80% aqueous ethanol (v/v). Slurry was centrifuged at 13,000*g* × 15 min at room temperature between consecutive extraction steps and the supernatants were combined. The yellow-colored extracts were filtered using 0.22 μm PVDF disposable syringe filters (Millex, Millipore, Badford, MA, USA) and stored at − 20 °C until analysis. At least five replicate extracts were prepared for each sample.

2.3. Total polyphenols

The concentration of total phenols (TPC) in the extracts was determined by the Folin-Ciocalteu colorimetric method, using the general procedures recommended by the European Pharmacopoeia for the determination of total tannins (European Directorate for the Quality of Medicines, 2007), monitoring the absorbance at 760 nm with a UV–vis spectrophotometer (Amersham Ultrospec 2100 Pro UV/Vis, GE Healthcare, Uppsala, Sweden). Gallic acid within the 50–500 mg/L concentration range was used as the standard. TPC was expressed as mg/g of SGF, taking into account the molar ratio between gallic acid and isoschaftoside (the most abundant component in all the extracts). Samples were assayed in triplicate and values were averaged.

2.4. RP-HPLC

SGF extracts were separated using a modular HP 1100 chromatographer (Agilent Technologies, Paolo Alto, CA, USA) equipped with a diode array detector (DAD). The stationary phase was a 250 × 2.0 mm i.d. C18 reversed-phase column, 4 μm particle diameter (Jupiter Phenomenex, Torrance, CA, USA). The column temperature was maintained at 37 °C during the HPLC analyses. Runs were performed at a constant flow rate of 0.2 mL/min applying a 5–60% linear gradient of the solvent B (acetonitrile/0.1% TFA) after 5 min of isocratic elution at 5% B. Solvent A was 0.1% TFA in HPLC-grade water. For each analysis, 10 μL of combined extracts 10-fold diluted with 0.1% TFA were injected. Samples were run in triplicate, at least. DAD was set-up to acquire an UV–vis spectra every second between 200 and 600 nm The HPLC separations were monitored at wavelengths λ = 520, 360, 320 and 280 nm.

To confirm the presence of non-hydrolyzable sugar moieties, aliquots of the extracts (from 100 mg SGF) were dried in a glass tube and suspended in 1 mL of 4N HCl. After 1 h at 50 °C, the solution was neutralized with 1 mL of 4N NaOH and freeze-dried. Finally, the yellowish residue was suspended in 3 mL methanol and analyzed by RP-HPLC as described, injecting 10 μL of the resulting solution 10-fold diluted with 0.1% TFA.

2.5. MALDI-TOF MS analysis

Off-line matrix assisted laser desorption ionization-time of flight (MALDI-TOF) MS analysis of manually collected RP-HPLC peaks was carried out in order to associate the RP-HPLC peaks to those of the nanoflow-HPLC ESI MS/MS analysis. MALDI-TOF MS spectra were acquired using a Voyager DE-Pro (PerSeptive Biosystems, Framingham, MA, USA), in both the positive and negative reflector ion modes using 2,5-dihydroxybenzoic acid (DHB) as the matrix (10 mg/mL in 50% ACN, v/v), according to previously detailed conditions (Picariello, De Vito, Ferranti, Paolucci, & Volpe, 2016). Typically, the *m/z* 400–1500 range was explored. The positive and negative mass ranges were externally calibrated with a mixture of standard polyphenols including quercetin-glucoside, malvidin 3,5-O-diglucoside and rutin (all from Sigma-Aldrich) mixed at a concentration 1 pmol/μL each in methanol.

2.6. Nanoflow-HPLC ESI MS/MS analysis

Nanoflow-HPLC ESI MS/MS analyses were performed using an Ultimate 3000 ultra-high performance liquid chromatography instrument (Dionex/Thermo Scientific, San Jose, CA, USA) online coupled with a Q-Exactive Orbitrap (Thermo Scientific) mass spectrometer. The SGF extracts were 10-fold diluted in 0.1% (v/v) formic acid solution and 1 μL of the resulting solution was loaded through a 5 mm long, 300 μm i.d. pre-column (LC Packings, USA) using a Famos (Dionex/Thermo Scientific) autosampler. Separation was performed on an EASY-Spray™ PepMap C18 column (2 μm, 15 cm × 75 μm) 3 μm particles, 100 Å pore size (Thermo Scientific), integrated with an in-source emitter tip heated at 250 °C and set at a 2.4 and 2.0 kV capillary voltage for the positive and negative mode, respectively. No auxiliary gas was used for the electrospray ionization. Eluent A was 0.1% formic acid (v/v) in water; eluent B was 0.1% formic acid (v/v) in acetonitrile. The column was equilibrated at 5% B. Components were separated applying a 4–40% linear gradient of B over 40 min at a flow rate of 300 nL/min. The mass spectrometer operated in data-dependent acquisition, switching between positive and negative ionization modes in 1 s and scanning the 300–1600 *m/z* range. The mass range was externally calibrated using the Calmix® standard and the ESI negative ion calibration solution (both from Pierce/Thermo) for the positive and negative ion modes, respectively. Mass accuracy of the Orbitrap measurement in the explored *m/z* range was better than 2 ppm. Up to 5 most intense ions in MS1 were selected for fragmentation in MS/MS mode. Mono-charged ions were selected for fragmentation provided that $m/z > 350$ and ion intensity $> 5.0 \times 10^6$. A resolving power of 70,000 full width at half maximum (FWHM), an automatic gain control (AGC) target of 1×10^6 ions and a maximum ion injection time of 100 ms were set to generate precursor spectra. MS/MS fragmentation spectra were generated with stepped fragmentation energy within 15–25 units at a resolving power of 17,500 FWHM. A dynamic exclusion of 10 s was applied for the MS/MS selection. Spectra were elaborated using the Xcalibur! Software 3.1 version (Thermo Scientific). Accuracy in the measurement of molecular weight was lower than 2 ppm. For the sake of briefness and practicality, molecular weight values of compounds are reported with one decimal figure and fragments approximated to the closest integer.

2.7. Semi-quantitative analysis

Semi-quantitative determination of most abundant glycosides was obtained by RP-HPLC operating in the conditions described above. Authentic apigenin dissolved in methanol was used as an external standard to construct a calibration curve in the 0.01–0.1 μg/μL concentration range ($R^2 = 0.991$). RP-HPLC peaks were integrated at baseline using the HPLC ChemStation software vers. A.07.01 (Agilent Technology) furnished with the chromatographer. Peak purity was assessed using a specific tool of the ChemStation software, operating of the basis of the UV-spectra obtained with DAD. No correction was applied in the case of co-elution of the main flavonoids with minor amounts of other components. Three runs for each point were carried out and data were statistically elaborated using the Microsoft Excel 2013 software. Semi-quantitative estimation has been performed on molar basis, taking into account the molecular weight of the most abundant component in the peaks, in the case of co-elution of two or more compounds.

2.8. Nomenclature of fragment ions

The nomenclature of fragment ions is adapted from (Cavaliere, Foglia, Pastorini, Samperi, & Laganà, 2005; Guo et al., 2013). The symbol $^{k,l}X_n$ and $^{k,l}Y_n$ detonate fragments still containing the intact aglycone; the superscripts "*k*" and "*l*" indicate the cleaved bonds within the carbohydrate rings. The subscripts "n" indicate the number of intact sugar rings still bound to the aglycone.

3. Results

3.1. RP-HPLC-DAD

The RP-HPLC chromatograms of the extracts from the four algarrobo/carob SGF samples are compared in Fig. 1. The RP-HPLC patterns are dominated by a component at retention time (t_r) 28.6 min (peak no. 6), whose UV–vis spectrum was characterized by two λ_{max} values, at 270 and 337 nm (inset of Fig. 1-I), compatible with a flavone molecular structure. *P. alba* and *P. nigra* SGF samples had almost identical RP-HPLC profiles, while *P. ruscifolia* revealed minor differences. In contrast, the *C. siliqua* SGF extracts contained a series of additional compounds, including the peak no. 1 at t_r 21.8 and the prominent components eluting at t_r 23.1 (no. 2) and at 24.1 (no. 3), which were much less represented in *Prosopis* spp. extracts. The retention time of the most abundant component (peak no. 6) did not shift after acidic hydrolysis suggesting that it was not an *O*-glycoside derivative. On the contrary, the low-abundant earlier eluting compounds of *C. siliqua* (peaks no. 2 and 3) were drastically reduced by acidic hydrolysis, indicating the occurrence of possible *O*-glycosides or interglycosidic-*O*-linkages.

3.2. HPLC-MALDI-TOF MS and nanoflow HPLC-ESI-MS/MS identification of major glycosides

The MALDI-TOF MS off-line analysis of RP-HPLC isolated phenolic compounds did not allow unambiguously assigning components. Thus, the extracts were analyzed by nanoflow-RP-HPLC coupled to high resolution MS/MS. The total ion current (TIC) chromatograms of the four extracts, including both positive and negative ion mode analyses, are compared in Fig. 2. As expected, the chromatographic patterns resembled those already observed in RP-HPLC DAD separation (cfr. Fig. 1). Compounds identified by nanoflow-HPLC ESI-MS/MS were associated to the corresponding narrowbore RP-HPLC peaks based on the elution order and on the molecular weight of the components, which in the case of RP-HPLC analysis was measured by off-line MALDI-TOF MS.

The molecular weight of the most abundant compound (HPLC peak no. 6) was $[M + H]^+$ 565.1/$[M - H]^-$ 563.1. Its fragmentation patterns were typical of a *C*-glucosylated flavonoid, showing repeated loss of 18 mass units in the positive ion mode and characteristic fragments arising from glycoside cross-ring cleavages, including $[(M - H) - 60]^-$ ($[^{0,4}X_0 - H]^-$ ion), $[(M - H) - 90]^-$ ($[^{0,3}X_0 - H]^-$ ion) and $[(M - H) - 120]^-$ ($[^{0,2}X_0 - H]^-$ ion) at 503, 473 and 443, respectively, in the negative ion mode (Fig. 3. MS/MS of peak no. 6). Indeed, as previously described, *C*-glycosides undergo typical fragmentation events and can be differentiated straightforwardly from isobaric *O*-glycosides through second order mass spectra (MS/MS) (Cavaliere et al., 2005). For instance, the unfragmented protonated molecule $[M + H]^+$ is generally of very low intensity in the MS/MS spectra of *O*-conjugates, while the loss of sugar moieties produces a

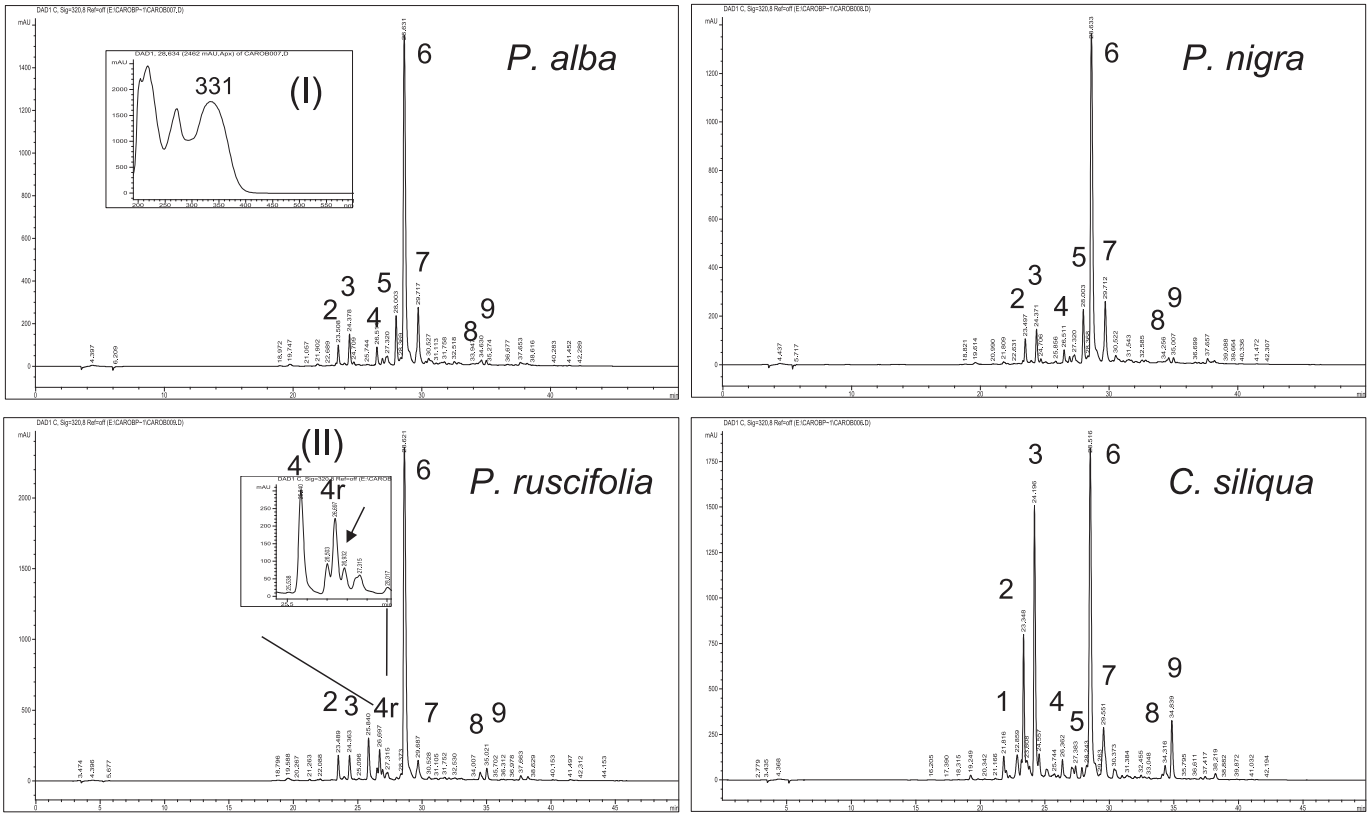

Fig. 1. RP-HPLC DAD comparison of polyphenols from *Prosopis* spp. and *C. siliqua* germ. UV absorption at λ = 330 nm is shown. The inset (I) in the upper left panel displays the UV spectrum of peak no. 6. Inset (II) is an enlarged view of the region of the chromatogram of *P. ruscifolia* extract. Peak no. 4r is a apigenin 6,8-*C*-di-glycoside isomer, practically exclusive of *P. ruscifolia*, which in contrast does not contain peak no. 5. The arrow indicates the small peak of luteolin 6,8-*C*-di-glcucoside, occurring in all the extracts.

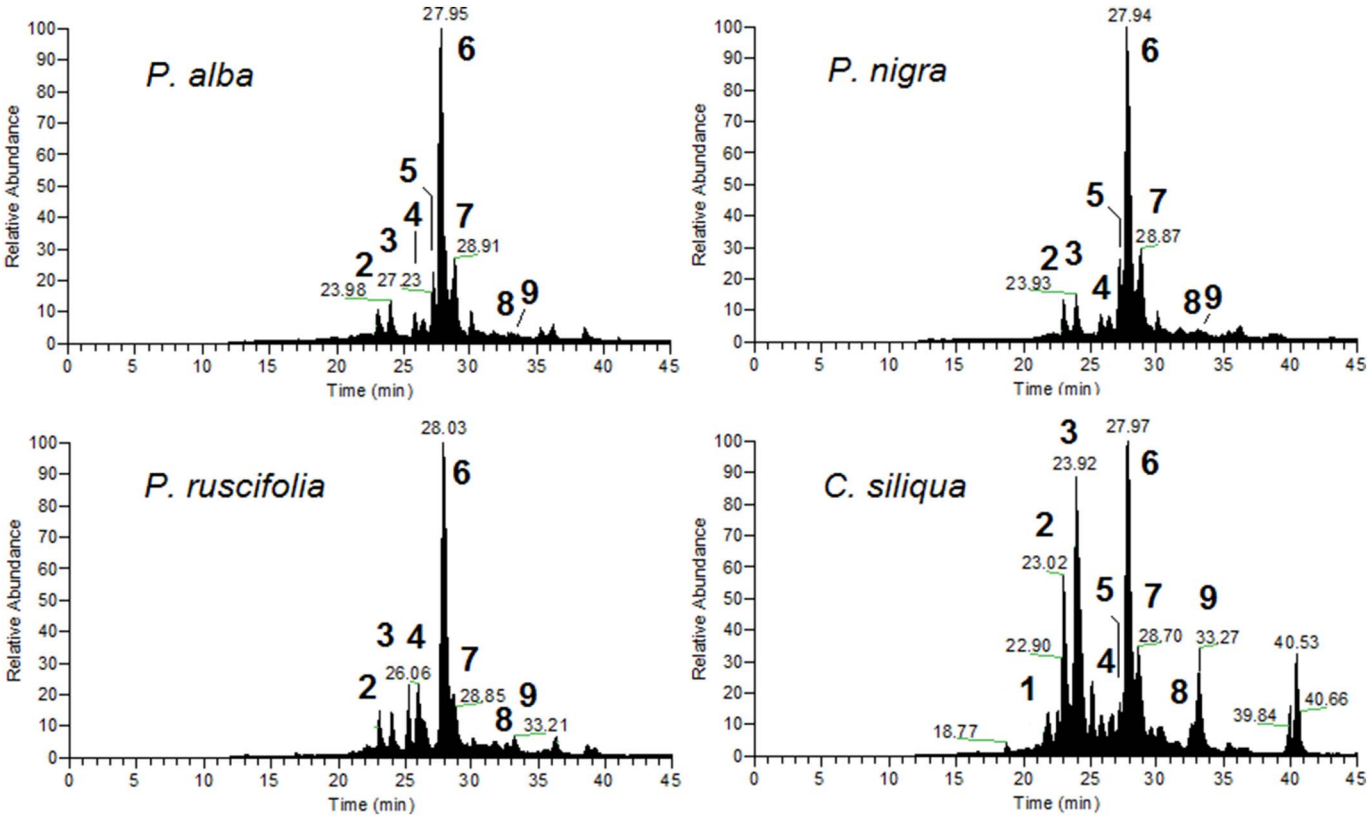

Fig. 2. Nanoflow-HPLC-ESI MS/MS comparative analysis of polyphenol extracts from *Prosopis* spp. and *C. siliqua*. Chromatograms are combined positive/negative TIC. Peak labels have been associated to those of the RP-HPLC DAD chromatograms (cfr. Fig. 1) through the molecular weight of the components and comparing the elution order.

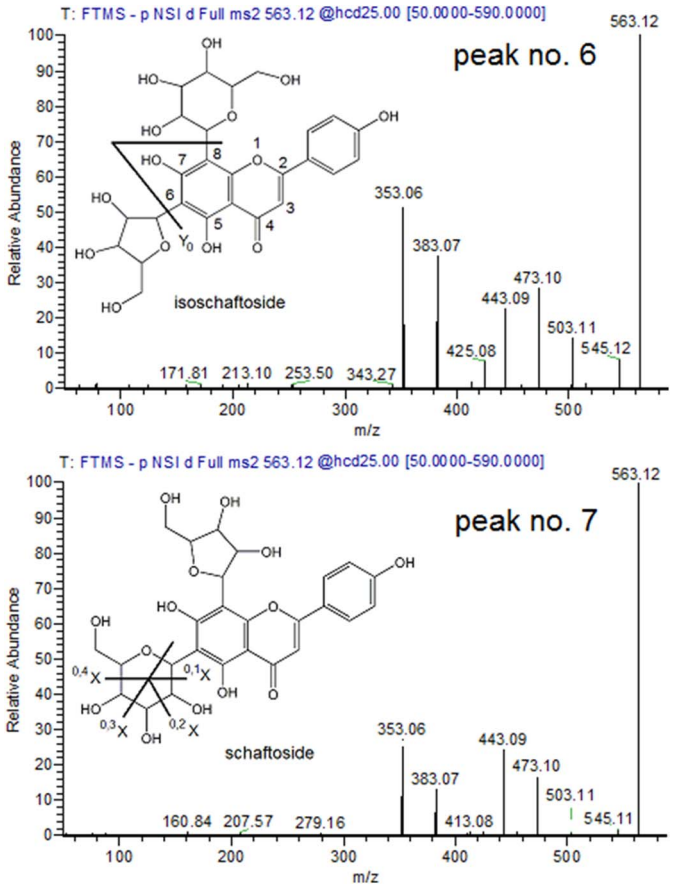

Fig. 3. Comparative analysis of the negative ion mode MS/MS fragmentation of isobaric compounds with $[M - H]^-$ = 563.1 in peak no. 6 (upper panel) and peak no. 7 (lower panel). Based on the intensity of the diagnostic $[(M - H) - 60]^-$ fragment ion and on the RP-HPLC elution order, compounds in peaks no. 6 and no. 7 were isoschaftoside and schaftoside, respectively. The main fragmentation routes which can involve *C*-glycosides are schematized in the insets, exemplified for the schaftosides.

prominent aglycone Y_0^+ ion signal. In the case of di-*O*-glycosides, the loss of only one sugar moiety also produces a relevant intermediate Y_1^+ ion. In contrast, the MS/MS spectra of *C*-glycosides spectra generally exhibit intense $[M + H]^+$ ion, with multiple loss of water molecules producing $[(M + H) - n18]^+$ signals. The Y_0^+ signal of the algycone is generally missing. Typical losses from the protonated molecule are 90, 120 and 150 Da units in the cases of hexose residues, 60 and 90 Da for pentose residues, and 74 and 104 Da for deoxyhexose residues.

The compound in peak no. 6 exhibited fragments characteristic of both hexose and pentose glycosides. The nature of the aglycone (A) was inferred from the specific A + 83 and A + 113 negative fragments ($[^{0,2}X_i\ ^{0,3}X_j]^-$ and $[^{0,2}X_i\ ^{0,2}X_j]^-$ ions, respectively), arising from simultaneous cross-ring cleavages within the two glycoside moieties (Becchi & Fraisse, 1989; Ferreres, Silva, Andrate, Seabra, & Ferreira, 2003). Thus, the molecule was identified as the asymmetric 6,8-di-*C*-glycosyl apigenin (flavone aglycone M = 270.1) conjugated with both a pentose and an hexose moiety. Consistently, the UV spectrum of the compound matched that of standard apigenin. The HPLC peak no. 7 contained an isobaric compound with $[M + H]^+$ 565.1 / $[M - H]^-$ 563.1, with fragmentation patterns strictly related to those of the compound in peak no. 6 (Fig. 3. MS/MS of peak no. 7).

In mono-*C*-glycosyl flavones, the fragment $[^{0,3}X_0 - H]^-$ ($[(M - H) - 60]^-$) is diagnostic, distinguishing the occurrence of a pentose from possible hexose conjugates. This fragment is expected in both the combinations of asymmetric 6,8-di-*C*-glycosyl flavones containing pentose and hexose moieties. However, the $[(M - H) - 60]^-$ fragment ion is more intense when the pentose is localized in the 6-*C* position than in the 8-*C* position (Becchi & Fraisse, 1989). Similarly, the fragments corresponding to $[M - H - H_2O]^-$ are more intense for 6-*C*-pentosyl derivative, due to stronger hydrogen bonding between the 2″ hydroxyl group of the sugar and 5- and/or 7-hydroxy groups of the aglycone, which promotes water elimination (Guo et al., 2013). Based on these considerations and on the elution order in RP-HPLC (Ferreres et al., 2003; Pérez et al., 2014), compounds in peaks no. 6. and no. 7 were identified as 6-*C*-pentosyl-8-*C*-glucosyl apigenin (isoschaftoside) and 6-*C*-glucosyl-8-*C*-pentosyl apigenin (schaftoside), respectively. Negative ion mode MS/MS spectra of isoschaftoside and schaftoside are compared in Fig. 3. The hexose and the pentose moieties have been assigned to glucose and arabinose by analogy with similar compounds already identified in several *Leguminosae* (Benayad, Gómez-Cordovés, & Es-Safi, 2014), also including carob cotyledons (Batista & Gomez, 1993) and *Prosopis* spp. pods (Pérez et al., 2014). However, the identity of the hexose and pentose should be confirmed by specific analysis of sugar moieties. The structure of the schaftosides and the main fragmentation routes are reported in the insets of Fig. 3.

3.3. Identification of minor glycosides

A number of additional glycosides was detected by RP-HPLC and HPLC-MS, as summarized in Table 1. Most of the glycosides of *C. siliqua* also occurred in *Prosopis* spp. extracts, although at lower abundance. RP-HPLC peaks no. 2 and 3, particularly prominent in *C. siliqua*, were tri-glycoside derivatives of apigenin with $[M + H]^+$ 727.2 and $[M - H]^-$ 725.2.

Tri-glycosides might be 6,8-di-*C*-glycosydes containing an additional *O*-glycosylation at the level of any of the phenol OH groups or, alternatively, derivatives containing a *C*-(*O*-glycosyl)-glycosyl moieties carrying an *O*-interglycosidic linkage. Recently, both these classes of compounds have been described in the alcohol extracts of wheat germ (Geng, Harnly, & Chen, 2015a). The respective structures have been elucidated by HPLC coupled to ion trap MS^n. Base peak in the MS/MS spectra of *O*-glycosylated flavonoids is generated by the breakdown of the *O*-glycoside moiety directly linked to the aglycone. In our case, the fragment at $[M - H]^-$ 563, though present, was not the most prominent, indicating the occurrence of a *C*-(*O*-glycosyl)-glycosyl di-saccharide unit. Thus, the compounds were tentatively identified as apigenin 6-*C*-(6″-*O*-glucosyl) arabinosyl-8-*C*-glucoside (peak no. 2) and apigenin 6-*C*-glucosyl-8-*C*-(6″glucosyl) arabinoside (peak no. 3).

In analogy with the compounds described in wheat germ, we assigned the *O*-interglycosidic bond to the 6″ hydroxyl of the *C*-linked sugar, although positions other than 6″ can be involved in the linkage (Geng et al., 2015a). An additional isobaric pair of isomers containing one *C*-(6″-*O*-glycosyl) glycoside and one arabinoside moiety is possible. In fact, we detected two more isobaric molecules with $[M + H]^+$ 727.2 and $[M - H]^-$ 725.2, as minor species in peak no. 1. These latter tri-glycosides were detected in *Prosopis* samples only at a trace level. Although they have been tentatively assigned in Table 1 based on their relative t_r, the exact identification of the four isomers was not possible only with MS/MS data.

The presence of an additional sugar was consistent with the early chromatographic elution in RP-HPLC as well as with the almost complete disappearance of the relevant HPLC peaks after acidic hydrolysis (data not shown). As expected, the conjugation with sugar moieties did not induced significant modification of the UV spectra, compared to apigenin aglycone (data not shown).

Trace amounts of two isobaric tetra-glycoside apigenin derivatives with $[M + H]^+$ 889.2 and $[M - H]^-$ 887.2, roughly eluting at the t_r of peak no. 1, were identified in both *C. siliqua* and *Propopis* spp. samples. The corresponding MS/MS spectra contained a fragment ion at 563 ($[M - H]^-$), suggesting that they might contain tri-glycoside moieties bound at 6-*C* or 8-*C* flavone positions, or two disaccharide moieties bound at each of the 6,8-*C* positions of apigenin. In Table 1 they have been indicated simply as apigenin tetra-saccharides.

Table 1
Assignment of the seed germ polyphenols based on nanoflow-HPLC ESI-MS/MS spectra. Peak numbers define the correspondence of compounds with RP-HPLC peaks (Fig. 1) and nanoflow-HPLC-ESI MS/MS analysis (Fig. 2). However, individual components are more accurately located with the t_r in nanoflow-HPLC-ESI MS/MS analysis. Compounds evidenced in bold are those predominant in the respective HPLC fraction. Diagnostic fragments are evidenced in bold. [a](w) = weak. n.f. = not fragmented; s = peak shoulder. Peak 4r is not reported because it was exclusive of *P. ruscifolia*.

Peak no.	Retention time (t_r)	$[M + H]^+$	$[M + H]^+$ fragments − positive ion mode	$[M - H]^-$	$[M - H]^-$ fragments − negative ion mode	Assignment
1	20.92	757.2	739, 721, 619, 541, 457, 379, 355	755.2	665, 653, **593**, 545, 515, 383, 353	Apigenin 6-*C*-(6″-O-glc) glc-8-*C*-glc
	21.64	727.2	709, 691, 673, 643, 589, 571, 511, 427, 409, 355	725.2	635, 605, **563**, 545, 515, 383, 353	Apigenin 6-*C*-(6″-*O*-glc) glc-8-*C*-arab
		889.2 (w)[a]	871, 853, 781, 751, 709, 691, 673, 619, 589, 427	887.2	797, 767, **563**, 473, 443, 383, 353	Apigenin tetrasaccharide (3 hex, 1 pent)
		757.2	739, 721, 619, 541, 457, 379, 355	755.2	665, 653, **593**, 545, 515, 383, 353	Apigenin 6-*C*-glc-8-*C*-(6″-O-glc) glc
	22.50	727.2	709, 691, 673, 643, 589, 571, 511, 427, 409, 355	725.2	635, 605, **563**, 545, 515, 383, 353	Apigenin 6-*C*-arab-8-*C*-(6″-*O*-glc) glc
		889.2 (w)	871, 853, 781, 751, 709, 691, 673, 619, 589, 427	887.2	797, 767(s), **563**, 473, 443, 383, 353	Apigenin tetrasaccharide (3 hex, 1 pent)
2	23.02	727.2	709, 691, 673, 643, 589, 571, 511, 427, 409, 355	725.2	635, 605, **563**, 545, 515, 473, 443, 383, 353	**Apigenin 6-*C*-(6″-*O*-glc) arab-8-*C*-glc**
3	23.92	727.2	709, 691, 673, 643, 589, 571, 511, 427, 409, 355	725.2	635, 605, **563**, 545, 515, 473, 443, 383, 353	**Apigenin 6-*C*-glc-8-*C*-(6″-O-glc) arab**
	24.27	697.2 (w)	n. f.	695.2 (w)	635, 605, 545, **533**, 515, 473, 443, 353, 383	Apigenin 6-*C*-(6″-*O*-glc) arab-8-*C*-arab
	25.04	595.1 (w)	n. f.	593.1	517,503, 443, **431**, **401**, 353, 383, **269**	Apigenin 5-*O*-glc-7-*O*-glc
4	25.13	595.1	577, 559, 511, 457, 427, 409, 355	593.1	503(w), 473, 431, 383, 353	**Apigenin 6-*C*-glc-8-*C*-glc**
	25.29	581.2 (w)	n. f.	579.1 (w)	533, 401, 269	Not identified apigenin *O*-glycoside
	25.67	697.2 (w)	n. f.	695.1	635, 605, 545, **533**, 515, 473, 443, 353, 383	Apigenin 6-*C*-arab-8-*C*-(6″-O-glc) arab
	26.49	581.1	563, 545, 527, 485, 461, 443, 425, 413, 395	579.1	519, 489, 459, 431, **399**, **369**	Luteolin 6-*C*-arab-8-*C*-glc
5	26.76	565.1	547, 529, 511, 499, 481, 427, 409, 379, 355	563.1	545, **503**(s), **473**, 443, 383, 353	**Apigenin 6-*C*-pentoside-7-*C*-hexoside**
	27.19	565.1	457, **433**, **271**	563.1	503, **431**, **269**	**Apigenin 5-*O*-arab-7-*O*-glc**
	27.34	641.1 (w)	n.f.	639.1 (w)	431, 311(w), 269	Not identified apigenin *O*-glycoside
6	27.89	565.1	547, 529, 511, 499, 481, 427, 409, 379, 355	563.1	545, **503**(s), **473**, 443, 383, 353	**Apigenin 6-*C*-arab-8-*C*-glc (isoschaftoside)**
7	28.70	565.1	547, 529, 511, 499, 481, 427, 409, 379, 355	563.1	545(w), **503**(w), **473**, 443, 383, 353	**Apigenin 6-*C*-glc-8-*C*-arab (schaftoside)**
8	29.60	535.1	517, 499, 481, 469, 427, 409, 397, 379	533.1	473, 443, 383, 353	Apigenin 6-*C*-arab-8-*C*-pent
	30.25	549.1	531, 513, 495, 411, 393, 363	547.1	**487**, 457, 427, **367**, **337**	Chrysin 6-*C*-arab-8-*C*-glc
	30.40 (s)	579.1 (w)	n. f.	577.1 (w)	503, 457, 383, 353	Apigenin 6-*C*-deoxyhex-8-*C*-glc
	30.91	433.1	415, 397, 379, 367, 337,313	431.1	383, 353, 341, 311	Apigenin 6-*C*-glucoside (isovitexin)
	31.20 (s)	579.1 (w)	n. f.	577.1 (w)	503, 457, 383, 353	Apigenin 6-*C*-glc-8-*C*-deoxyhex
	31.55	549.1	531, 513, 495, 411, 393, 363	547.1	**487(w)**, 457, 427, **367**, **337**	Chrysin 6-*C*-glc-8-*C*-arab
	32.59	771.2	753, 735, 681, 651, 585, 531, 511, 385, 369	769.2	679, 649, **593(w)**, 575, 455, 353, 335	**Apigenin 6-*C*-feruloyl glc-8-*C*-glc**
	32.62	741.2	723, 705, 675, 585, 511, 427, 385	739.2	619, 577, **563(w)**, 545, 425, 353, 335	**Apigenin 6-*C*-feruloyl arab-8-*C*-glc**
9	33.34	741.2	723, 705, 675, 585, 511, 427, 385	739.2	619, 577, **563(w)**, 545, 425, 353, 335	**apigenin 6-*C*-feryloyl glc-8-*C*-arab**
	35.32	433.1	**271**	431.1	**269**	Apigenin *O*-glucoside

Peak no. 4 was the symmetric apigenin 6,8-*C*-di-glucoside (vicenin-2), with $[M + H]^+$ 595.1 and $[M - H]^-$ 593.1, which eluted earlier than the corresponding *C*-hexosyl-*C*-pentosyl glycosides. Vicenin-2 was fairly abundant in *P. ruscifolia* and *C. siliqua*, whereas it was much less represented in *P. alba* and *P. nigra*.

Two low abundance isobaric tri-glycoside derivatives of this latter compound, with $[M + H]^+$ 757.2 and $[M - H]^-$ 755.2, eluted at lower RP-HPLC t_r (in peak no. 1). They were apigenin 6-*C*-(6″-*O*-glycosyl) glycosyl-8-*C*-glycoside and 8-*C*-(6″-*O*-glycosyl) glycosyl-6-*C*-glycoside, showing the diagnostic fragment ion at *m/z* 593 in the negative MS/MS spectra. These tri-glicosides occurred at significant amount only in *C. siliqua*.

P. ruscifolia contained an additional peak with $[M + H]^+$ 595.1 and $[M - H]^-$ 593.1, indicated in Fig. 1 as 4r, which was missing in the other extracts. As the MS/MS spectra of the two isobaric components of *P. ruscifolia* were very similar, the compound in 4r might be a vicenin-2 isomer containing one (or both) hexose moiety other than glucose. A small peak eluting in *P. ruscifolia* near to 4r (Fig. 1, inset II, indicated by an arrow) and detected at much lower intensity in the other samples, was 6-*C*-arabinosyl-8-*C*-glucosyl luteolin. This glycoside had measured $[M + H]^+$ 581.1 and $[M - H]^-$ 579.1 and its negative ion MS/MS spectra exhibited diagnostic A + 83 and A + 113 fragments at *m/z* 369 and 399. The luteolin aglycone was confirmed by the UV–Vis spectrum with λ_{max} = 272 and 351 nm. Similarly, very weak signals of two 6,8-*C*-pentosyl-hexosyl derivatives of an aglycone containing an OH group less than apigenin ($[M + H]^+$ 549.1 and $[M - H]^-$ 547.1), probably chrysin, were detected in peaks no. 7 and no. 8. Isomeric chrysin 6-*C*-pentosyl-8-*C*-hexoside and 6-*C*-hexosyl-8-*C*-pentoside as indicated in Table 1 were discriminated through the fragment ion $[(M - H) - 60]^-$, as described above. These compounds were distinct from closely eluting apigenin 6,8-*C*-deoxyhexosyl-*C*-glucosyl derivatives, because of the A + 83 and A + 113 ion fragments in negative MS/MS (observed $[M - \ - H]^-$ 337.1 and 367.1).

Peak no. 5, practically missing in *P. ruscifolia*, contained an *O*-di-glycoside apigenin, most likely apigenin 5-O-arabinosyl-7-*O*-glucoside $[M + H]^+$ 565.1 / $[M - H]^-$ 563.1). Probably, a *C*-glycoside schaftoside isomer, containing a different epimer (for instance, corymboside, i.e. apigenin 6-*C*-arabynosil-8-*C*-galactoside) or a different anomeric linkage (*e.g.* neoschaftoside), co-eluted in this peak. The symmetric apigenin 5-*O*-glucosyl-7-*O*-glucoside ($[M + H]^+$ 595.1), exhibiting prominent signals corresponding to mono-glycoside Y_1^+ fragments and to the aglycone Y_0^+ (Fig. 4) was also identified at t_r 25.04 (Peak no. 3).

The symmetric 6,8-*C*-di-pentosyl apigenin ($[M + H]^+$ 535.1 and $[M - H]^-$ 533.1) as well as the pair of its further glycosylated derivatives ($[M + H]^+$ 697.2 and $[M - H]^-$ 695.2), were minor compounds eluting in peak no. 7 and in peaks no. 3 and no. 4 (Table 1), respectively.

Two compounds with $[M + H]^+$ 581.1 / $[M - H]^-$ 579.1 and $[M + H]^+$ 641.1 / $[M - H]^-$ 639.1 occurred at a very low amounts only in *C. siliqua* extracts. Most likely they were apigenin *O*-glycosides, as inferred by the strong aglycone fragment $[M - H]^-$ 269, but it was not possible to achieve their definitive identification.

Late eluting compounds in peaks no. 8 and 9. of *C. siliqua*, missing in the *Prosopis* spp. extracts, were tentatively identified as feruloyl acylated derivatives of vicenin-2 (peak no. 8, $[M + H]^+$ 771.2 and $[M - H]^-$ 769.2) and of isoschaftoside/schaftoside (peak no. 9, $[M + H]^+$ 741.2 and $[M - H]^-$ 739.2) based on MS spectra and UV absorbance profile (λ_{max} = 270 and 330 nm) as well as on their delayed elution. Low-abundance apigenin O-glucoside was also detected in all the extracts, though more intense in *C. siliqua*, eluting after peak no. 9. Based on the fragmentation pattern, this latter compound was distinct from isobaric apigenin *C*-glucoside (isovitexin) which eluted earlier at t_r 30.31.

The peaks detected by nanoflow-HPLC MS/MS at t_r 39.97 and 40.53 min in *C. siliqua* and much less in *Prosopis* samples were non-polyphenol compounds as they were not detected by HPLC-UV–Vis. They were digalactosyl diglycerides (DGDG) (e.g. DGDG, 18:2/18:2 $[M + H]^+$ 941.4 and $[M - H]^-$ 939.4) and relate glycolipids with molecular weight $[M + H]^+$ 927.4, 941.4, 971.4 and 985.4, which have been already identified in soft wheat germ (Geng et al., 2015a).

3.4. Semi-quantitative determination of C-glycosidic flavonoids

TPC of SGF, measured with the Folin-Ciocalteu method were within the 5.12–8.83 mg/g range, according to the following rank *C. siliqua* > *P. ruscifolia* > *P. nigra* > *P. alba* (Table 2). TPC were measured using gallic acid as the standard. In the calculation, it has been considered the molar ratio between gallic acid and isoschaftoside, selected as the reference flavonoid of SGF. TPC amount and rank were in line with those determined by RP-HPLC.

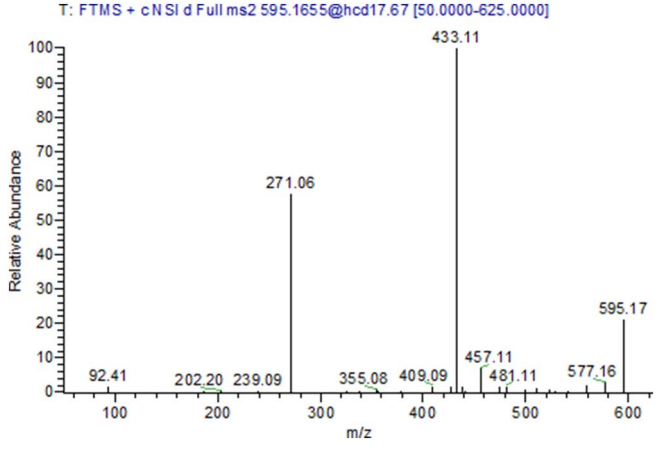

Fig. 4. MS/MS based identification of apigenin 5-O-glucosyl-7-O-glucoside ($[M + H]^+$ 595.1) at tr 25.04 min. The peak base fragment at $[M + H]^+$ 433.1 corresponds to the loss of a hexose moiety because of the cleavage of an *O*-glycoside bond. The loss of the second hexose unit produced a prominent signal fragment of the aglycone ($[M + H]^+$ 271.1).

Table 2
Folin-Ciocalteu determination of total phenol compounds and RP-HPLC-based semi-quantification of individual polyphenols in SGF extracts. Values are the mean of three independent determinations (technical replicates). Standard deviation was lower than 10% in all the cases.

		P. alba	*P. nigra*	*P. ruscifolia*	*C. siliqua*
TPC (Folin-Ciocalteu assay) [mg/g SGF]		5.12	5.82	7.26	8.83
RP-HPLC-based quantification of individual polyphenols					
Peak no.	Main compound	(mg/g SGF)			
2	Apigenin 6-*C*-(6″-O-glc) arab-8-*C*-glc[a]	0.24	0.29	0.32	1.18
3	Apigenin 6-*C*-glc-8-*C*-(6″-O-glc) arab[a]	0.35	0.38	0.35	2.44
4	Apigenin 6-*C*-glc-8-*C*-glc	0.19	0.18	0.51	0.23
4r	Apigenin 6-*C*-glc-8-*C*-glc isomer	/	/	0.39	/
5	Apigenin 5,7-O-diglucosides + apigenin 6-*C*-pentoside-7-*C*-hexoside	0.37	0.47	/	Low
6	Apigenin 6-*C*-arab-8-*C*-glc (isoschaftoside)	3.37	3.86	5.18	3.22
7	Apigenin 6-*C*-glc-8-*C*-arab (schaftoside)	0.61	0.72	0.41	0.66
8 + 9	Apigenin 6,8-*C*-di-glycoside feruloylated derivatives	Trace	Trace	Trace	0.61

[a] Isomers tentatively assigned.

The semi-quantitative composition of individual *C*-glycosidic flavones from algarrobo and carob SGF extracts was obtained by RP-HPLC. An external calibration curve was constructed in the 0.01–0.1 μg/μL concentration range (R^2 = 0.991), using apigenin as the standard. The individual amounts of the main *C*-glycoside flavonoids was obtained considering the molar ratio between each species and apigenin and are summarized in Table 2 as mg/g SGF. The flavonoid amounts determined in this work were quite lower than those recently found in *P. alba*, although within the same order of magnitude (Cattaneo et al., 2016). The accuracy of the determination of the major glycosides could be slightly biased due to the co-elution with other minor species (see Table 1). *P. ruscifolia* contained the highest amount of isoschaftoside, whereas *C. siliqua* contained relatively high levels of apigenin try-glycosides. Flavonoid composition of *P. alba* and *P. nigra* SGF was very similar, apart a slightly different level of schaftoside isomers.

4. Discussion

In this work, for the first time, the glycosylated flavonoids of SGF from three Argentinean algarrobo (*Prosopis* spp.) and one European carob (*C. siliqua*) species were comparatively characterized. The flavonoid composition of the samples was strictly related under a qualitative standpoint, confirming on a phenotypic basis the taxonomic parentages among the species. Nevertheless, *C. siliqua* contained significantly higher amounts of tri-glycosilated derivatives if compared to *Prosopis* spp. samples. Within the *Prosopis* family, flavonoid patterns of *P. alba* and *P. nigra* SGFs were almost identical, whereas *P. ruscifolia* showed minor differences.

In all the extracts, the most abundant components were apigenin 6,8-*C*-di-glycosides, namely isoschaftoside and schaftoside, with amounts within the 3.22–5.18 and 0.41–0.72 mg/g SGF ranges, respectively.

Isoschaftoside and schaftoside have been already described in algarrobo and carob pods as well as in a number of species belonging to the *Fabaceae* family, such as *Lespedeza capitata* (Linard, Delaveau, Paris, Dellamonica, & Chopin, 1982), *Desmodium* spp. (Hamilton et al., 2012), *Trigonella foenum-graecum* (Benayad et al., 2014) and *Securigera securidaca* (Ibrahim et al., 2015), where they function as phytoalexins.

Apigenin *C*-glycosides appear also quite widespread in several plant compartments of non-*Leguminosae* plants, many among which traditionally used in phytochemistry, such as *Passiflora* spp. (Li et al., 1991), *Triticum durum* (Cavaliere et al., 2005) and *Triticum aestivum* (Wojakowska, Perkowski, Góral, & Stobiecki, 2013), *Citrus* ssp. (Gattuso, Barreca, Gargiulli, Leuzzi, & Caristi, 2007), *Moraceae* (Omar, Mullen, & Crozier, 2011), *Violaceae* spp. (Cao, Yin, Qin, Cheng, & Chen, 2014; Vukics, Ringer, Kery, Bonn, & Guttman, 2008) and *Capsicum annum* (Materska, 2015). Apigenin *C*-glycosides have been also described as main polyphenol constituents of quince (*Cydonia oblonga*) seeds (Ferreres et al., 2003) and, interestingly, of soft wheat (*T. aestivum*) germ, so that they have been proposed as candidate markers to discriminate between whole-grain and refined wheat flour (Geng, Zhang, Harnly, Luthria, & Chen, 2015b).

In general, numerous flavonoids are reported to be inhibitors of glycohydrolases. Most likely, they physiologically contribute to modulate the hydrolysis of polysaccharides during seed quiescence and germination events, besides protecting the seed compartments from cellulases, xylanases and pectinases of pathogenic insects, pests and microorganisms (Mierziak, Kostyn, & Kulma, 2014). Accumulation of *C*-glycosidic flavones in carob and algarrobo seeds could be related to the relatively high amount of galactomannans (LBG). In particular, apigenin *C*-glycosides are strong α-glucosidase inhibitors, even more powerful than acarbose (Li et al., 2009), a tetra-saccharide drug used to delay the digestion and absorption of carbohydrates. By competitively hindering the digestion of complex saccharides, α-glucosidase inhibitors decrease the postprandial hyperglycemia. Therefore, *C*-glycosylated apigenin and congener flavonoids could supposedly exert positive effects on subjects suffering from type-2 diabetes mellitus (Yin, Zhang, Feng, Zhang, & Kang, 2014). Accessorial beneficial outcomes on diabetic syndrome arise from their antioxidant and platelet aggregation inhibitory activities. In general, the use or the incorporation of algarrobo and carob SGF in food formulations might provide an interesting alternative to prepare food products with reduced glycemic index. In this sense, *Prosopis* spp. germ flour could be more effective than the *C. siliqua* counterpart, due to a lower relative degree of apigenin glycosylation. In fact, the extensive glycosylation at *C*-6 or *C*-8 of the flavone weakens the α-glucosidase inhibitory potential, resulting in a less accentuated delay of polysaccharide digestion (Li et al., 2009).

A wide range of additional health-promoting effects, including anti-aging, anti-inflammatory, anti-bacterial, anti-parasitic and anti-tumor properties, have been associated to dietary flavonoid *C*-glycosides, as recently reviewed (Xiao, Muzashvili, & Georgiev, 2014).

Some of the bioactive properties of stingless bee honey have been attributed to apigenin *C*-glycosides. In these terms, the amount found in algarrobo and carob SGFs is relevant, considering that these molecules occur in stingless bee honey at much lower concentration (Truchado, Vit, Ferreres, & Tomas-Barberan, 2011). Noteworthy, apigenin *C*-glycosides do not exhibit mutagenic effects in vitro (Cattaneo et al., 2016).

Custódio et al. (2011) specifically studied the antioxidant and cytotoxic activity of methanol extracts from carob germ flour. These authors identified several phenolic acids by HPLC and attributed some of the bioactive properties observed to a relatively high concentration of theophylline, which had been already described as a minor component in water infusions of carob pods (Corsi et al., 2002). Although we have not specifically monitored theophylline, we did not find RP-HPLC peaks in the methanol extracts of *Prosopis* spp. or *C. siliqua* germ ascribable to it.

5. Conclusions

The structure of *C*-glycosylated flavonoid from *Prosopis* spp. and *C. siliqua* SGFs was elucidated by HPLC and high resolution MS/MS. Isoschaftoside and schaftoside were the most abundant components in all the extracts analyzed and occurred in relatively high amount. The supposed bioactive properties of flavone *C*-glycosides might complement the anti-oxidant, anti-inflammatory and anti-mutagenic effects attributed to proteins and protein hydrolizates, which have been reported for *Prosopis* spp. seed flour (Cattaneo et al., 2014). In this perspective, algarrobo and carob SGF is a candidate food ingredient, obtained from processing by-products of neglected crops, with potential health-promoting effects.

However, the benefits of apigenin *C*-glycosydes on human health, specifically anti-oxidant and anti-diabetic potential, still await to be confirmed with opportunely designed in vivo studies. Similarly, very few data are still available about their stability, pharmacodynamics and pharmacokinetics, though dedicated investigations have started to be undertaken very recently (Kandhare, Bodhankar, Mohan, & Thakurdesai, 2016).

Conflict of interest

The authors declared no conflict of interest.

Acknowledgement

The present investigation has been carried out in the framework of the CNR/CONICET (Italy/Argentina) bilateral research agreement 2015-2016 awarded to G. M. and M. C. P.

References

Avallone, R., Plessi, M., Baraldi, M., & Monzani, A. (1997). Determination of chemical composition of carob (*Ceratonia siliqua*): Protein, fat, carbohydrates, and tannins.

Journal of Food Composition and Analysis, *10*, 166–172.
Ayaz, F. A., Torun, H., Glew, R. H., Bak, Z. D., Chuang, L. T., Presley, J. M., & Andrews, R. (2009). Nutrient content of carob pod (*Ceratonia siliqua* L.) flour prepared commercially and domestically. *Plant Foods for Human Nutrition*, *64*, 286–292.
Batista, M. T., & Gomez, E. T. (1993). C-glycosylflavones from *Ceratonia siliqua* cotyledons. *Phytochemistry*, *34*, 1191–1193.
Becchi, M., & Fraisse, D. (1989). Fast Atom Bombardment and Fast Atom Bombardment collision-activated dissociation/mass-analysed ion kinetic energy analysis of C-glycosidic flavonoids. *Biomedical and Environmental Mass Spectrometry*, *18*, 122–130.
Benayad, Z., Gómez-Cordovés, C., & Es-Safi, N. E. (2014). Characterization of flavonoid glycosides from fenugreek (*Trigonella foenum-graecum*) crude seeds by HPLC-DAD-ESI/MS analysis. *International Journal of Molecular Sciences*, *15*, 20668–20685.
Bengoechea, C., Romero, A., Villanueva, A., Moreno, G., Alaiz, M., Millán, F., ... Puppo, M. C. (2008). Composition and structure of carob (*Ceratonia siliqua* L.) germ proteins. *Food Chemistry*, *107*, 675–683.
Bernardi, C., Sánchez, H., Freyre, M., & Osella, C. (2010). Gluten-free bread formulated with *Prosopis ruscifolia* (vinal) seed and corn flours. *International Journal of Food Sciences and Nutrition*, *61*, 245–255.
Bigne, F., Puppo, M. C., & Ferrero, C. (2016). Fibre enrichment of wheat flour with mesquite (*Prosopis* spp): Effect on breadmaking performance and staling. *LWT - Food Science and Technology*, *65*, 1008–1016.
Burkart, A. (1976). A monograph of the genus Prosopis (Leguminosae subfam. Mimosoideae). Part 1–2. *Journal of the Arnold Arboretum*, *57*, 219–249450-425.
Bush, V. M., Kolender, A. A., Santagapita, P. R., & Bluera, M. P. (2015). Vinal gum, a galactomannan from *Prosopis ruscifolia* seeds: Physicochemical characterization. *Food Hydrocolloids*, *51*, 495–502.
Cabrera, A. L. (1976). *Enciclopedia argentina de agricultura y jardinería. Fascículo 1, Regiones fitogeográficas argentinas*. Buenos Aires, Argentina: Acme.
Cao, J., Yin, C., Qin, Y., Cheng, Z., & Chen, D. (2014). Approach to the study of flavone di-*C*-glycosides by high performance liquid chromatography-tandem ion trap mass spectrometry and its application to characterization of flavonoid composition in *Viola yedoensis*. *Journal of Mass Spectrometry*, *49*, 1010–1024.
Cattaneo, F., Costamagna, M. S., Zampini, I. C., Sayago, J., Alberto, M. R., Chamorro, V., ... Isla, M. I. (2016). Flour from *Prosopis alba* cotyledons: A natural source of nutrient and bioactive phytochemicals. *Food Chemistry*, *208*, 89–96.
Cattaneo, F., Sayago, J. E., Alberto, M. R., Zampini, I. C., Ordoñez, R. M., Chamorro, V., ... Isla, M. I. (2014). Anti-inflammatory and antioxidant activities, functional properties and mutagenicity studies of protein and protein hydrolysate obtained from *Prosopis alba* seed flour. *Food Chemistry*, *161*, 391–399.
Cavaliere, C., Foglia, P., Pastorini, E., Samperi, R., & Laganà, A. (2005). Identification and mass spectrometric characterization of glycosylated flavonoids in *Triticum durum* plants by high-performance liquid chromatography with tandem mass spectrometry. *Rapid Communications in Mass Spectrometry*, *19*, 3143–3158.
Choge, S., Pasiecznik, N., Harvey, M., Wright, J., Awan, S. Y., & Harris, P. (2007). *Prosopis* pods as human food, with special reference to Kenya. *Water SA*, *33*, 419–424.
Corsi, L., Avallone, R., Cosenza, F., Farina, F., Baraldi, C., & Baraldi, M. (2002). Antiproliferative effects of *Ceratonia siliqua* L. on mouse hepatocellular carcinoma cell line. *Fitoterapia*, *73*, 674–684.
Custódio, L., Escapa, A. L., Fernandes, E., Fajardo, A., Aligué, R., Alberício, F., ... Romano, A. (2011). Phytochemical profile, antioxidant and cytotoxic activities of the carob tree (*Ceratonia siliqua* L.) germ flour extracts. *Plant Foods for Human Nutrition*, *66*, 78–84.
Dakia, P. A., Wathelet, B., & Paquot, M. (2007). Isolation and chemical evaluation of carob (*Ceratonia siliqua* L.) seed germ. *Food Chemistry*, *102*, 1368–1374.
European Directorate for the Quality of Medicines. Council of Europe (2007). Determination of tannins in herbal drugs. *European Pharmacopoeia*(6th ed.). France: Strasbourg (p. A286).
Ferreres, F., Silva, B. M., Andrate, P. B., Seabra, R. M., & Ferreira, M. A. (2003). Approach to the study of *C*-glycosyl flavones by ion trap HPLC–PAD–ESI/MS/MS: Application to seeds of quince (*Cydonia oblonga*). *Phytochemical Analysis*, *14*, 352–359.
Freyre, M., Astrada, E., Blasco, C., Baigorria, C., Rozycki, V., & Bernardi, C. (2003). Valores nutricionales de frutos de vinal (*Prosopis ruscifolia*): Consumo humano y animal. *Ciencia y Tecnologia Alimentaria*, *4*, 41–46.
Gattuso, G., Barreca, D., Gargiulli, C., Leuzzi, U., & Caristi, C. (2007). Flavonoid composition of *Citrus* juices. *Molecules*, *12*, 1641–1673.
Geng, P., Harnly, J. M., & Chen, P. (2015a). Differentiation of whole grain from refined wheat (*T. aestivum*) flour using lipid profile of wheat bran, germ, and endosperm with UHPLC-HRAM mass spectrometry. *Journal of Agricultural and Food Chemistry*, *63*, 6189–6211.
Geng, P., Zhang, M., Harnly, J., Luthria, D., & Chen, P. (2015b). Use of fuzzy chromatography mass spectrometric (FCMS) fingerprinting and chemometric analysis for differentiation of whole-grain and refined wheat (*T. aestivum*) flour. *Analytical and Bioanalytical Chemistry*, *407*, 7875–7888.
Guo, X., Yue, Y., Tang, F., Wang, J., Yao, X., & Sun, J. (2013). A comparison of *C*-glycosidic flavonoid isomers by electrospray ionization quadrupole time-of-flight tandem mass spectrometry in negative and positive ion mode. *International Journal of Mass Spectrometry*, *333*, 59–66.
Hamilton, M. L., Kuate, S. P., Brazier-Hicks, M., Caulfield, J. C., Rose, R., Edwards, R., ... Hooper, A. M. (2012). Elucidation of the biosynthesis of the di-*C*-glycosylflavone isoschaftoside, an allelopathic component from *Desmodium* spp. that inhibits *Striga spp.* development. *Phytochemistry*, *84*, 169–176.
Ibrahim, R. M., El-Halawany, A. M., Saleh, D. O., El-Naggar, M. B., El-Shabrawy, R. O., & El-Hawary, S. S. (2015). HPLC-DAD-MS/MS profiling of phenolics from *Securigera securidaca* flowers and its anti-hyperglycemic and anti-hyperlipidemic activities. *Revista Brasileira de Farmacognosia*, *25*, 134–141.
Kandhare, A. D., Bodhankar, S. L., Mohan, V., & Thakurdesai, P. A. (2016). Development and validation of HPLC method for vicenin-1 isolated from fenugreek seeds in rat plasma: Application to pharmacokinetic, tissue distribution and excretion studies. *Pharmaceutical Biology*, *54*, 2575–2583.
Karim, A. A., & Azlam, A. (2012). Fruit pod extracts as a source of nutraceuticals and pharmaceuticals. *Molecules*, *17*, 11931–11946.
Li, H., Song, F., Xing, J., Tsao, R., Liu, Z., & Liu, S. (2009). Screening and structural characterization of α-glucosidase inhibitors from hawthorn leaf flavonoids extract by ultrafiltration LC-DAD-MSn and SORI-CID FTICR MS. *Journal of the American Society for Mass Spectrometry*, *20*, 1496–1503.
Li, Q. M., van den Heuvel, H., Delorenzo, O., Corthout, J., Pieters, L. A., Vlietinck, A. J., & Claeys, M. (1991). Mass spectral characterization of C-glycosidic flavonoids isolated from a medicinal plant (*Passiflora incarnata*). *Journal of Chromatography*, *562*, 435–446.
Linard, A., Delaveau, P., Paris, R. R., Dellamonica, G., & Chopin, J. (1982). Isocarlinoside, a di-*C*-glycosylflavone from *Lespedeza capitate*. *Phytochemistry*, *21*, 797–799.
Materska, M. (2015). Flavone *C*-glycosides from *Capsicum annuum* L.: Relationships between antioxidant activity and lipophilicity. *European Food Research and Technology*, *240*, 549–557.
Mierziak, J., Kostyn, K., & Kulma, A. (2014). Flavonoids as important molecules of plant interactions with the environment. *Molecules*, *19*, 16240–16265.
Omar, M. H., Mullen, W., & Crozier, A. (2011). Identification of proanthocyanidin dimers and trimers, flavone *C*-glycosides, and antioxidants in *Ficus deltoidea*, a malaysian herbal tea. *Journal of Agricultural and Food Chemistry*, *59*, 1363–1369.
Pérez, M. J., Cuello, A. S., Zampini, I. C., Ordoñez, R. M., Alberto, M. R., Quispe, C., ... Isla, M. I. (2014). Polyphenolic compounds and anthocyanin content of *Prosopis nigra* and *Prosopis alba* pods flour and their antioxidant and anti-inflammatory capacities. *Food Research International*, *64*, 762–771.
Picariello, G., De Vito, V., Ferranti, P., Paolucci, M., & Volpe, M. G. (2016). Species- and cultivar-dependent traits of *Prunus avium* and *Prunus cerasus* polyphenols. *Journal of Food Composition and Analysis*, *45*, 50–57.
Salinas, M. V., Carbas, B., Brites, C., & Puppo, M. C. (2015). Influence of different carob fruit flours (*Ceratonia siliqua* L.) on wheat dough performance and bread quality. *Food and Bioprocess Technology*, *8*, 1561–1570.
Saunders, R. M., & Becker, R. (1989). Development of *Prosopis* species leguminous trees as an agricultural crops. In G. E. Wickens, & N. Haq (Eds.), *New crops for food and industry* (pp. 288–301). Cambridge, UK: Day P. Chapman and Hall Publisher.
Sciammaro, L. P., Ferrero, C., & Puppo, M. C. (2016b). Chemical and nutritional properties of different fractions of *Prosopis alba* pods and seeds. *Journal of Food Measurement and Characterization*, *10*, 103–112.
Sciammaro, L. P., Ribotta, P. D., & Puppo, M. C. (2016a). Traditional food products from *Prosopis* sp. flour. In K. Kristbergsson, & J. Oliveira (Vol. Eds.), *Traditional foods. General and consumer aspects. ISEKI Food Series. Vol. 10. Traditional foods. General and consumer aspects. ISEKI Food Series* (pp. 209–216). Springer.
Srivastava, M., & Kapoor, V. P. (2005). Seed galactomannans: An overview. *Chemistry & Biodiversity*, *2*, 295–317.
Truchado, P., Vit, P., Ferreres, F., & Tomas-Barberan, F. (2011). Liquid chromatography-tandem mass spectrometry analysis allows the simultaneous characterization of *C*-glycosyl and *O*-glycosyl flavonoids in stingless bee honeys. *Journal of Chromatography A*, *1218*, 7601–7607.
Villagra, P., Cony, M. A., Mantován, N. G., Rossi, B. E., González-Loyarte, M., Villalba, R., et al. (2004). Ecología y manejo de los algarrobales de la Provincia Fitogeográfica del Monte. In M. F. Arturi, J. L. Frangi, & J. F. Goya (Eds.), *Ecología y Manejo de Bosques Nativos de Argentina*. Argentina: Editorial Universidad Nacional de La Plata.
Vukics, V., Ringer, T., Kery, A., Bonn, G. K., & Guttman, A. (2008). Analysis of heartsease (*Viola tricolor* L.) flavonoid glycosides by micro-liquid chromatography coupled to multistage mass spectrometry. *Journal of Chromatography A*, *1206*, 11–20.
Wojakowska, A., Perkowski, J., Góral, T., & Stobiecki, M. (2013). Structural characterization of flavonoid glycosides from leaves of wheat (*Triticum aestivum* L.) using LC/MS/MS profiling of the target compounds. *Journal of Mass Spectrometry*, *48*, 329–339.
Xiao, J., Muzashvili, T. S., & Georgiev, M. I. (2014). Advances in the biotechnological glycosylation of valuable flavonoids. *Biotechnology Advances*, *32*, 1145–1156.
Yin, Z., Zhang, W., Feng, F., Zhang, Y., & Kang, W. (2014). α-Glucosidase inhibitors isolated from medicinal plants. *Food Science and Human Wellness*, *3*, 136–174.
Yousif, A. K., & Alghzawi, H. M. (2000). Processing and characterization of carob powder. *Food Chemistry*, *69*, 283–287.